Journal of Pharmacokinetics and Pharmacodynamics (2025) 52:33
https://doi.org/10.1007/s10928-025-09971-w

ORIGINAL PAPER

Interplay between pharmacokinetics and immunogenicity of therapeutic proteins: stepwise development of a bidirectional joint pharmacokinetics-anti-drug antibodies model

Jan-Stefan van der Walt[1] · Justin Wilkins[1] · Akash Khandelwal[2] · Karthik Venkatakrishnan[3] · Wei Gao[3] · Ana-Marija Milenković-Grišić[2]

Received: 6 December 2024 / Accepted: 27 March 2025

Abstract

The aim of the analysis was to develop a phenomenological longitudinal population pharmacokinetics (PK)-anti-drug antibodies (ADA) model to enable an informed and quantitative framework for assessment of ADA influence. Data used were from seven clinical studies of avelumab across drug development phases in patients with several tumor types. ADA as covariate in a population PK model, and Markov models of ADA status (ADA+ or ADA−) were investigated. Finally, a joint PK-ADA model was developed. In the population PK models that evaluated ADA as a covariate, the clearance increase attributable to ADA+ status was 8.5% (time-varying ADA) to 19.9% (time-invariant ADA with inter-occasion variability in clearance). With a discrete-time Markov model (DTMM), tumor type was identified as a significant covariate on the probability of ADA− to ADA+ transition. When ADA time course predicted by the DTMM model was implemented as a covariate in the population PK model, an increase in avelumab clearance of 11–41% was estimated depending on tumor type. With a continuous-time Markov model (CTMM), in addition to tumor type, baseline ADA status was identified to significantly influence the ADA− to ADA+ transition rate constant. The joint PK-CTMM model estimated the maximal increase in CL due to ADA as 15% and a decrease in ADA− to ADA+ transition rate of up to 37% with increasing avelumab concentration, with 50% of the maximum decrease occurring at 349 μg/mL. The present work established a framework for the assessment of interactions between PK and immunogenicity for therapeutic proteins.

✉ Ana-Marija Milenković-Grišić
ana-marija.milenkovic@emdgroup.com

[1] Occams, Amstelveen, The Netherlands

[2] The Healthcare Business of Merck KGaA, Darmstadt, Germany

[3] EMD Serono, Billerica, MA, USA

Published online: 21 May 2025

Graphical Abstract

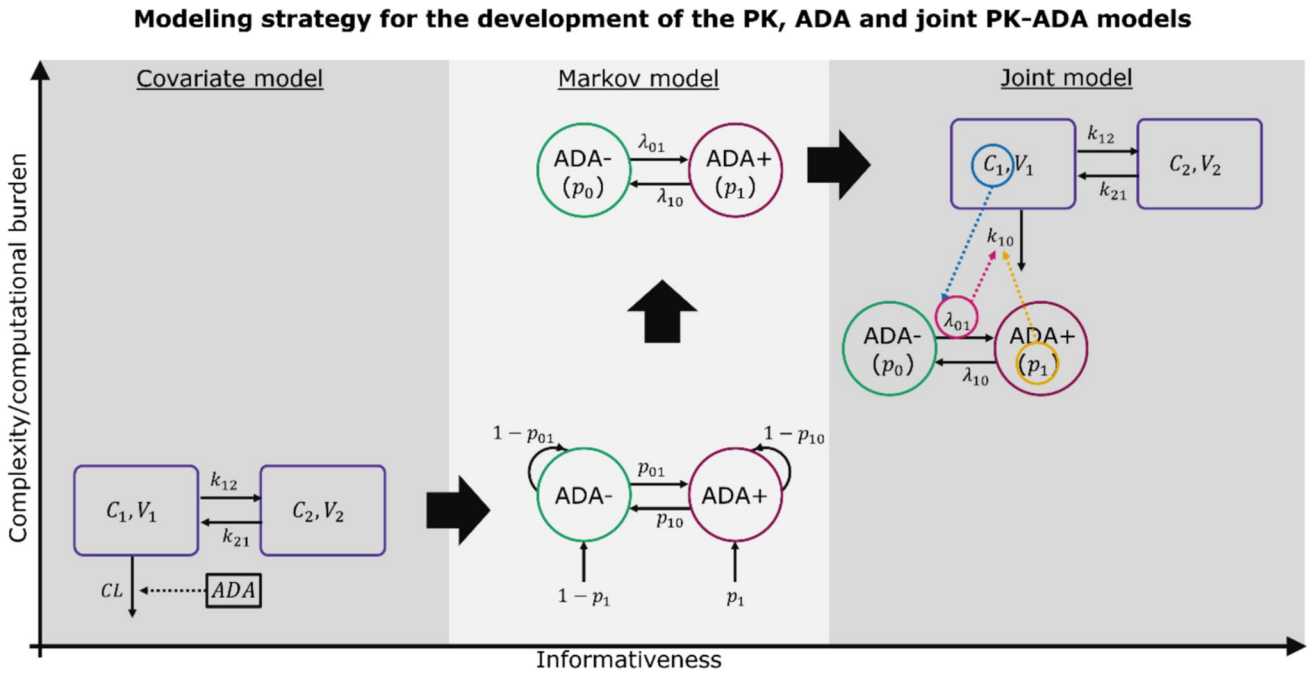

ADA = anti-drug antibody; C_1 = plasma concentration associated with central compartment; C_2 = plasma concentration associated with peripheral compartment; λ_{01} = rate to transition from ADA- to ADA+ status; λ_{10} = rate to transition from ADA+ to ADA- status; p_0 = probability of ADA- status; p_1 = probability of ADA+ status; p_{01} = probability to transition from ADA+ to ADA- status; p_{01} = probability to transition from ADA- to ADA+ status; V_1 = volume of distribution of the central compartment; V_2 = volume of distribution of the peripheral compartment.

Keywords Therapeutic proteins · Immunogenicity/anti-drug antibodies · Bidirectional model · Avelumab

Introduction

Immunogenicity, the development of anti-drug antibodies (ADA), is an important characteristic of therapeutic proteins, affecting pharmacokinetics (PK) and pharmacodynamics (PD), including drug efficacy and safety [1, 2]. Immunogenicity is an inherent characteristic of therapeutic proteins, resulting from natural immune processes, but ADA development can also be influenced by intrinsic and extrinsic factors such as the underlying disease and its status, or comedication with immune system-altering drugs, such as corticosteroids, immunomodulators, or chemotherapy [3, 4].

Mechanistically, all ADA form immune complexes with drug molecules which are subsequently eliminated, thereby increasing the clearance of the drug to varying extents. At the same time, ADA (especially neutralizing ADA, which bind to target-binding sites on the drug molecule) can inhibit drug molecules binding to their targets, thus potentially negating the pharmacological activity of the drug, in addition to lowering its exposure owing to increased clearance (CL). ADA-drug immune complexes can also cause anaphylactic/hypersensitivity reactions. For cancer immunotherapies, it has been proposed that development of ADA might be a surrogate marker of immune system activation and therefore drug efficacy [2].

Due to the complexity inherent in ADA (different IgG classes, only semi-quantitative analytical methods, and an array of other complications), the kinetics of ADA development are difficult to characterize [5]. The effects of ADA on PK, efficacy, and safety of drugs are often investigated by classifying patients as ADA+ (developed ADA at any point during the trial) or ADA− (never developed ADA during the trial) in a time-constant manner. This way, valuable information is lost, whereas modeling ADA structurally and in a time-varying manner would reduce this information loss by enabling the use of ADA information over time. Furthermore, assigning ADA status on patient level (ADA ever/never) is pharmacologically not appropriate for describing causal relationships and additionally introduces immortal-time bias [6], as this non-baseline variable is treated as known

at baseline, thereby confounding the results of such analyses. The fact that ADA are commonly reported as titers, not absolute concentrations, further complicates analysis in a quantitative mechanistic manner. Finally, simulations with ADA are typically not feasible in the absence of a model describing their development.

Published population models that account for ADA usually include overall ADA status (ever/never or, less frequently, ADA as a time-varying covariate) as a covariate on CL or volume of distribution (V), not as a part of a structural model [7]. Further, many approaches are limited to accounting only for patients who develop ADA and are not suitable for describing ADA− patients. While limitations inherent to the observed ADA data (such as having only titers available) cannot be fully circumvented, a longitudinal PK-ADA model would theoretically enable an informed and less biased framework for assessment of ADA influence.

Avelumab is a human immunoglobulin G1 (IgG1) anti-programmed death ligand 1 (PD-L1) monoclonal antibody [8] with a wild-type fragment crystallizable (Fc) region, indicated as monotherapy for the treatment of adult patients with metastatic Merkel cell carcinoma (MCC), first-line maintenance treatment of adult patients with locally advanced or metastatic urothelial carcinoma (UC) who are progression-free following platinum-based chemotherapy, and in combination with axitinib for first-line treatment of adult patients with advanced renal cell carcinoma (RCC) [9].

The overall aim of this investigation was to develop a bidirectional joint PK-ADA model on an immuno-oncology data set to establish a framework for assessing the impact of immunogenicity on drug PK. As the first step, within this project, two alternative approaches to account for ADA were investigated: (1) ADA as a time-varying covariate in a population PK model, and (2) a Markov model of ADA status linked to a population PK model. Markov models are mathematical models that describe systems which transition from one state to another, with the probability of each transition depending only on the current state and not on the previous states [10].

Apart from the interaction between systemic drug concentrations and ADA status, the ADA status analysis included investigating covariate effects on ADA status transitions. Potential effects of tumor type were also investigated within the covariate analysis.

Methods

Data

The analysis was performed using pooled data of patients treated with avelumab across drug development phases with different oncology indications from multiple clinical trials. An overview of the analyzed patient population is given in Table 1. Data from 1892 patients with evaluable PK data were used in the analysis and were split into two subsets stratified by ADA incidence (ever vs never ADA+): a subset for model development (1513 patients, ~ 80% of data) and a validation subset (379 patients, ~ 20% of data). Previously, a population PK model developed on data from 3 of the 7 clinical trials was published [11].

Avelumab concentrations were quantified using an immunoassay sandwich method (interrun coefficient of variation [CV] ≤ 16.1%, bias [absolute value] ≤ 15.5%, total interrun error ≤ 19.1%). The lower limit of quantification was 0.2 µg/mL [11]. ADA testing was conducted using a tiered assay approach, whereby samples that were screened and confirmed positive for ADA were subsequently analyzed to determine the titer using the homogeneous bridging electro chemiluminescent immuno-assay [12]. The following numbers of data points/participants were used for the model development and evaluation: PK development, 12,707/1513; PK evaluation, 3362/377; CTMM development, 14,874 /1495; CTMM evaluation, 3925/375; DTMM development, 14,247/1513; and DTMM evaluation, 3766/378. The average number of ADA samples and collection times are provided in Table 1. Missing ADA data were ignored in the analyses. There was no minimum ADA data requirement for a patient to be considered evaluable. Only 7 patients with neutralizing antibody were reported, and for 76 data points, the neutralizing antibody information was missing.

Avelumab population PK model

A previously-developed population PK model for avelumab formed the basis for PK-ADA model development [11]. This model was 2-compartmental, with time-dependent clearance (CL; Fig. 4). Decrease in CL was modeled as a sigmoid maximal inhibitory response process [13]:

$$CL_{i,t} = TVCL \cdot \exp\left(\frac{I_{max,i} \cdot t_i^{\gamma}}{T_{50}^{\gamma} + t_i^{\gamma}}\right) \cdot \exp(\eta_{CL,i})$$

Here, $CL_{i,t}$ is CL in individual i at time t, $TVCL$ is the typical value of CL in the population, $I_{max,i}$ is the maximal possible change in CL relative to baseline for individual i, t_i is the time after first dose in individual i, T_{50} is the time at which 50% of I_{max} is reached, γ describes the shape of the relationship, and $\eta_{CL,i}$ is interindividual variability (IIV) in CL for individual i, defined as being normally distributed with a mean of 0 and variance of ω_{CL}^2. In addition to CL, IIV was included on central volume of distribution (V1) and I_{max} (additively for the latter). The residual error was described by a combined additive and proportional error model. For the current analysis all covariate effects were

Table 1 Summary of clinical data included in the analysis

Study	JAVELIN Solid Tumor	JAVELIN Solid Tumor JPN	JAVELIN Merkel 200	JAVELIN Lung 200	JAVELIN Lung 100	JAVELIN Gastric 100	JAVELIN Gastric 300
Description	Avelumab in metastatic or locally advanced solid tumors (UC cohorts)	Avelumab in metastatic or locally advanced solid tumors	Avelumab in 2L Merkel cell carcinoma	Avelumab in 2L NSCLC	Avelumab in 1L NSCLC	Avelumab in 1L maintenance gastric cancer	Avelumab in 3L gastric cancer
Phase	I/Ib	I	II	III	III	III	III
ClinicalTrials.gov ID	NCT01772004	NCT01943461	NCT02155647	NCT02395172	NCT02576574	NCT02625610	NCT02625623
Indication	2L UC	Solid tumors in Japanese patients; expansion in GC	2L MCC	2L NSCLC	1L NSCLC	1L GC/GEJC	3L GC/GEJC
Dosing regimen(s)	10 mg/kg Q2W	3 mg/kg Q2W, 10 mg/kg Q2W, 20 mg/kg Q2W	10 mg/kg Q2W	10 mg/kg Q2W	10 mg/kg Q2W or 10 mg/kg Q1W for 12 weeks then 10 mg/kg Q2W	10 mg/kg Q2W	10 mg/kg Q2W
Number of patients included in the analysis	249	57	88	393	688	233	184
Patients ever ADA+ in the analyzed data set (%)	7.6	8.8	5.7	13.0	15.3	9.0	9.2
Number of ADA samples (sampling days)	8 (0, 14, 28, 42, 56, 60, 84, 168)	3 (14, 28, 42)	5 (0, 14, 28, 42, 84)	8 (0, 14, 28, 42, 84, 124, 168, 252)	17 (0, 28, 42, 56, 84, 140, 168, 252, 336, 420, 504, 558, 672, 756, 850, 924, 1008)	7 (0, 14, 28, 42, 84, 124, 168)	5 (0, 14, 28, 42, 84)

1L first line, *2L* second line, *3L* third line, *GC* gastric cancer, *GEJC* gastroesophageal junction cancer, *MCC* Merkel cell carcinoma, *NSCLC* non-small cell lung cancer, *Q2W* every two weeks, *Q1W* every week, *UC* urothelial carcinoma

removed except body weight as a covariate on CL and V1 using standard allometry coefficients [14].

Joint PK-ADA model

Two approaches to model ADA data were investigated: (1) ADA as a covariate in the population PK model, and (2) Markov models of ADA status. Finally, a PK-ADA model linked the Markov model for ADA status to the population PK model to assess the bidirectional effect of ADA status on PK and drug exposure on ADA status simultaneously. The modeling strategy started with model development for models with lower complexity/computational burden and progressed to models with higher complexity/computational burden. ADA status was evaluated for effect on avelumab PK as a categorical covariate on avelumab clearance using different categorizations of ADA status: ADAEVER (time-invariant, ever vs never ADA+), ADAONCE (time-varying, ADA+ at first appearance of ADA and thereafter), and ADALOCF (time-varying, ADA+ vs ADA−) as graphically demonstrated in Fig. 1.

The ADA part of the joint model was considered be Markovian in nature, since it is likely to depend on state transitions over time: ADA− to ADA+, and back again, based on the previous state, and on time. ADA status was modeled using two-state discrete-time (DTMM) and two-state continuous-time (CTMM) Markov models. The Markov ADA-models were evaluated using VPCs for both the probability of ADA status as well as the probability to change ADA state or to remain in the same ADA state. Covariate relationships identified for the DTMM were included in the CTMM. The joint PK-ADA model was constructed by linking the population PK model to the CTMM to assess the effects of ADA on avelumab clearance and the effect of avelumab exposure on ADA status.

Discrete-time Markov models

Discrete-time Markov models (DTMMs) assume time to be a discrete variable, the recorded observation times in a clinical study. DTMM equations describe the transition probability from state k_{j-1} to state k_j, or more simply, the probability of each state k_j at the current occasion j given that state k_{j-1} was observed at the previous occasion $j-1$ [15].

The DTMM (Fig. 2) may be summarized as follows:

$$P_{01,i,j} = P(Y_{i,j} = 1 | Y_{i,j-1} = 0)$$

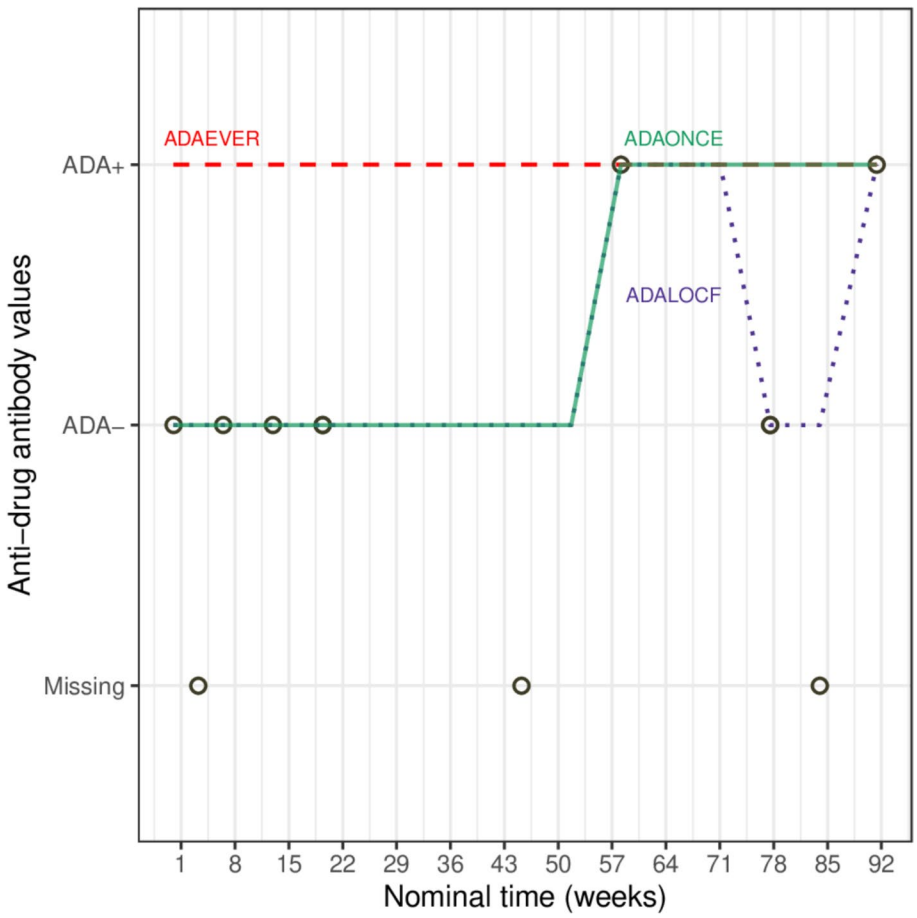

Fig. 1 Categories of time-variant ADA, using a representative patient

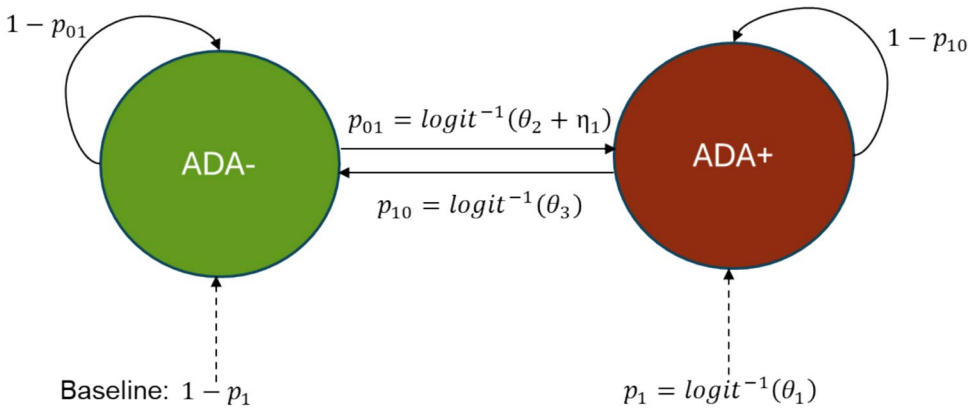

Fig. 2 Structure of the discrete-time Markov model. p_{10} : probability to transition from ADA+ to ADA−; $\boldsymbol{p}_{01}$: probability to transition from ADA− to ADA+

$$P_{00,i,j} = P\left(Y_{i,j} = 0 | Y_{i,j-1} = 0\right) = 1 - P_{01,i,j}$$

$$P_{10,i,j} = P(Y_{i,j} = 0 | Y_{i,j-1} = 1)$$

$$P_{11,i,j} = P(Y_{i,j} = 1 | Y_{i,j-1} = 1) = 1 - P_{10,i,j}$$

Here, P_{01} is the probability of a transition from ADA− (state 0) to ADA+ (state 1) in individual i at observation occasion j, P_{10} is the probability of a transition from ADA+ to ADA− in individual i at observation occasion j, $P_{00,i,j}$ is the probability that ADA remains negative in individual i at observation occasion j, and $P_{11,i,j}$ is the probability that ADA remains positive in individual i at observation occasion j. $Y_{i,j}$ is the observed value of ADA (+ or −) in individual i at observation occasion j, while $Y_{i,j-1}$ is the observed value of ADA (+ or −) in individual i at preceding observation occasion $j-1$.

The probabilities were estimated using a logit transformation:

$$P_{01,i} = \frac{1}{\left(1 + \exp\left(-\left(TVP_{01} + \eta_{P_{01}}\right)\right)\right)}$$

Here, $P_{01,i}$ is the individual realization of patient i's probability to transition from ADA− to ADA+ where TVP_{01} is the typical value of the probability in the population, and $\eta_{P_{01}}$ is the IIV defined as being normally distributed with a mean of 0 and variance of $\omega^2_{P_{01}}$.

Continuous-time Markov models

The continuous-time Markov model (CTMM) is more appropriate for non-uniform observation times, although for two-state data, the DTMM and CTMM methods may produce similar results for naturally discretized data (e.g. prespecified time points based on clinical trial designs) [10]. In this method, the influence of the previous state on the probability of the current state typically decreases with increasing time between observations [16–18].

$$P_{00,i,j} = \frac{\lambda_{10,i} + \lambda_{01,i} \cdot e^{-\left(\lambda_{10,i} + \lambda_{01,i}\right) \cdot \Delta t_{i,j}}}{\lambda_{01,i} + \lambda_{10,i}}$$

$$P_{01,i,j} = 1 - P_{00,i,j}$$

$$P_{11,i,j} = \frac{\lambda_{01,i} + \lambda_{10,i} \cdot e^{-\left(\lambda_{10,i} + \lambda_{01,i}\right) \cdot \Delta t_{i,j}}}{\lambda_{01,i} + \lambda_{10,i}}$$

$$P_{10,i,j} = 1 - P_{11,i,j}$$

Here, $\lambda_{01,i}$ is the transfer rate constant from state 0 to state 1 in individual i, $\lambda_{10,i}$ is the transfer rate constant from state 1 to state 0 in individual i, and $\Delta t_{i,j}$ is the time difference between the current and previous observations in individual i at observation occasion j. Other parameters are as previously defined. Treatment and covariate effects can be applied to λ_{01} and λ_{10}.

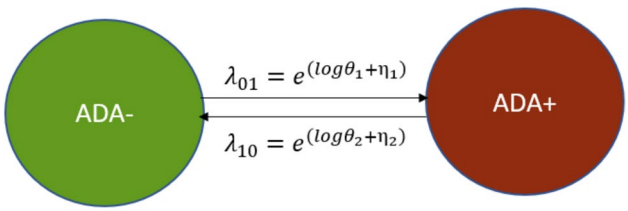

$$\frac{\delta A_0}{\delta t} = -\lambda_{01} \cdot A_0 + \lambda_{10} \cdot A_1$$

$$\frac{\delta A_1}{\delta t} = \lambda_{01} \cdot A_0 - \lambda_{10} \cdot A_1$$

Fig. 3 Structure of the continuous-time Markov model (CTMM). λ_{10}: rate constant for ADA+ to ADA− transition; λ_{01}: rate constant for ADA− to ADA+ transition; $A1$: probability for ADA+; $A0$: probability for ADA−

In the current case, the CTMM was implemented as ordinary differential equations (ODEs) representing the probabilities of ADA being negative or positive (Fig. 3):

$$\frac{dA_0}{dt} = -\lambda_{01} \cdot A_0 + \lambda_{10} \cdot A_1$$

$$\frac{dA_1}{dt} = \lambda_{01} \cdot A_0 - \lambda_{10} \cdot A_1$$

A_0 and A_1 represent the probabilities of ADA being negative and positive, respectively. Using this approach, modifications to the data file were necessary to facilitate analysis with NONMEM (version 7.4.3) [19]; compartment amounts and associated bioavailability values were reset after each observation [18]. Aside from ADA status itself, covariates on ADA state transition probabilities were considered, particularly tumor type. The transition rates were estimated using a log transformation:

$$\lambda_{01,i} = exp^{(logTV_{\lambda_{01}} + \eta_{\lambda 01})}$$

Here, $\lambda_{01,i}$ is the individual realization of patient i's transition rate from ADA− to ADA+ where $TV_{\lambda_{01}}$ is the typical value of the transition rate in the population and $\eta_{\lambda_{01}}$ is the IIV defined as being normally distributed with a mean of 0 and variance of $\omega^2_{\lambda_{01}}$.However, the data did not support the estimation of IIV in λ_{01} or λ_{10}.

The joint PK-ADA model combined the base population PK model (without ADA effect or IOV) with the final CTMM (including covariates). The models were linked by (1) estimating the correlation between avelumab clearance and λ_{01}, (2) effect of probability of ADA+ status ($p1$) on clearance (mono-directional joint PK-ADA model), and (3) time-course of the effect of avelumab exposure on the λ_{01} and the effect of $p1$ on clearance (bi-directional joint PK-ADA model). The typical values of avelumab clearance, λ_{01}, and the associated IIV parameters were estimated. All other parameters were fixed to the final typical values of the estimates of the base population PK model and the final CTMM.

The bi-directional effects are demonstrated in Fig. 4. The effect of $p1$ on avelumab CL ($P1_{eff,i}$) was modeled as a linear

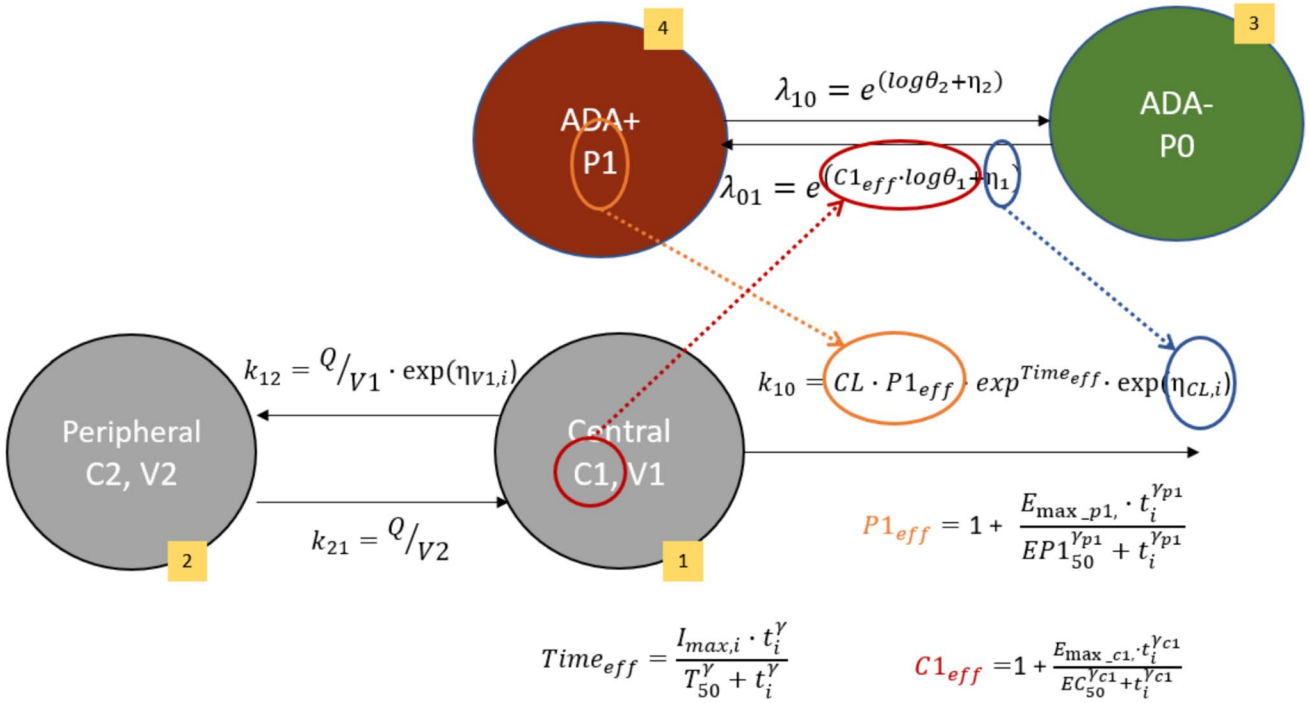

Fig. 4 Structure of the bidirectional joint PK-ADA model. CL: clearance; Q: intercompartmental clearance; V1: central volume of distribution; V2: peripheral volume of distribution; $P1_{eff}$: effect of probability of ADA+on CL; $C1_{eff}$: effect of concentration in central compartment on probability of ADA+; $Time_{eff}$: effect of time on CL; I_{max}: maximum change in CL relative to baseline; T_{50}: time for half of maximum effect; γ : shape of time effect curve; E_{max_c1}: maximum change in effect of exposure on rate of transition from ADA− to ADA+; EC_{50}: concentration for half of maximum exposure effect; γ_{c1}: shape of exposure effect curve; E_{max_p1}: maximum change in CL due to ADA; $EP1_{50}$: probability of ADA+for half of maximum ADA effect; γ_{p1}: shape of the ADA effect curve; λ_{10}: rate constant for ADA+to ADA− transition; λ_{01}: rate constant for ADA− to ADA+transition; $p1$: probability for ADA+; $p0$: probability for ADA−

or as a non-linear relationship between $p1$ (independent variable) and CL (dependent variable):

$$k_{10,i} = \frac{CL_i}{V1_i} \cdot P1_{eff,i} \cdot e^{(Time_{eff} + \eta_{CL,i})}$$

$$P1_{eff,i} = 1 + sl \cdot p1_i \quad \text{(linear model)}$$

$$P1_{eff,i} = 1 + \frac{E_{\max\_P1} \cdot p1_{t,i}^{\gamma_{P1}}}{EP_{50}^{\gamma_{P1}} + p1_{t,i}^{\gamma_{P1}}} \text{(non-linear model)}$$

Here, $k_{10,i}$, CL_i, and $V1_i$ are the avelumab elimination rate constant from the central compartment, avelumab CL, and central volume of distribution, respectively, for patient i. In the linear model the intercept is set to 1 (no change) and sl is the slope of change in $p1$. The nonlinear model is a sigmoidal Emax model, and $E_{\max\_P1}$ and EP_{50} are the maximum effect and 50% of the maximum effect of $p1$ on clearance. γ^{CP1} describes the shape of the relationship.

The link model for the relationship between exposure and rate of ADA transition ($C1_{eff}$) is a sigmoidal Emax model:

$$\lambda_{01,i} = e^{(C1_{eff,i} \bullet log\theta_{\lambda 01} + \eta_{\lambda 01})}$$

$$C1_{eff,i} = 1 + \frac{E_{\max\_C1\bullet} C1_{t,i}^{\gamma_{C1}}}{EC_{50}^{\gamma_{C1}} + C1_{t,i}^{\gamma_{C1}}}$$

Here, $C1_{t,i}$ is avelumab concentration in the central compartment in individual i at time t, $E_{\max\_C1\bullet}$ is the typical value of the maximal possible change in λ_{01} relative to baseline, EC_{50} is the typical value of the concentration at which 50% of $E_{\max\_C1\bullet}$ is reached, and γ^{C1} describes the shape of the relationship. The direction of the maximum change (i.e. an increase or a decrease) was not specified but was limited to a range of − 100% to 500%.

Covariate model

Potential covariate relationships were explored graphically by plotting the potential covariates versus the parameters of interest. Graphical exploration procedures were only relied upon if the degree of η-shrinkage in the parameters was reasonably low (< 30%) [20].

Covariate analysis for the population PK model was restricted to the relationship between the different categorizations of ADA status (ADAEVER, ADAONE, ADALOCF, etc.) and avelumab CL. The ADA-CL relationship was implemented using a linear function:

$$CL_i = TVCL \cdot \left(1 + \theta_{ADA}\right)$$

Here, CL_i is CL in individual i, $TVCL$ is the typical value of CL in the population, and θ_{ADA} is the estimated of change in CL when ADA+. For the DTMM and CTMM, covariate relationships included demographics (age, sex, and race), disease-related status (serum albumin, C-reactive protein [CRP], Eastern Cooperative Oncology Group performance score [ECOG] status, tumor type, and baseline tumor burden), previous and current concomitant therapies (previous use of biologics or PD-L1 inhibitors), and baseline laboratory results and organ function (aspartate transaminase [AST], alanine transaminase [ALT], creatinine, creatinine clearance, bilirubin, estimated glomerular filtration rate [eGFR]). Categorical covariates were tested using a linear function and continuous covariates were tested using power functions (see below).

Covariate model development was performed stepwise (using the stepwise covariate modeling tool in Perl-speaks-NONMEM [PsN], version 5.3.0) [21, 22]. Each candidate covariate was tested on each of the parameters of interest, one at a time. The parameter-covariate relationship producing the largest change in the NONMEM objective function value (OFV) was retained. This process was repeated as a series of forward model-building steps until no further parameter-covariate relationships were present that met the forward inclusion criterion (a change in OFV of − 3.843, corresponding to a nominal significance level of p = 0.05). A backward elimination process was then undertaken, in which each relationship was removed one at a time. At each backward step, the parameter-covariate relationship with the lowest change in OFV and not meeting the backward elimination criterion (a change in OFV of + 10.83, corresponding to a nominal significance level of p = 0.001) was removed. The process was concluded when no further parameter-covariate relationships could be removed.

The testing of categorical covariates was implemented using a linear function, as follows:

$$PARCOV_i = PAR_i \cdot \left(1 + \theta_{PAR,COV,val}\right)$$

where $PARCOV_i$ is the parameter value for individual i, PAR_i is the typical value of the parameter in the population, and $\theta_{PAR,COV,val}$ is an estimated parameter corresponding to the unique value of the categorical covariate in individual i. For the largest or reference category, $\theta_{PAR,COV}$ was defined as 0. Covariate categories containing less than 20 patients were not separately tested (except for tumor type) but instead lumped with the reference case (typically the category with highest frequency in the population).

Testing of continuous covariates was performed using a power function, as follows:

$$PARCOV_i = PAR_i \cdot \left(\frac{COV_i}{\overline{COV}}\right)^{\theta_{PAR,COV}}$$

where $PARCOV_i$ and PAR_i are as previously defined, COV_i is the value of the covariate in individual i, $\overline{COV}$ is the median value of the covariate in the population, and $\theta_{PAR,COV}$ is a parameter describing the shape of the relationship of the covariate to the parameter.

Model evaluation and qualification

Stratification was used when appropriate to ensure that the model could be evaluated adequately across important subgroups of the data. The adequacy of the models was evaluated using visual predictive checks (VPC) [23]. The population PK and PK-ADA models were used to simulate 500 replicates (model development) or 1000 replicates (external validation) of the analysis data set. Statistics of interest were calculated from the simulated and observed data for comparison: the 2.5th, 50th (median), and 97.5th percentiles of the distributions of the simulated concentration at each sampling time bin were calculated. These percentiles of the simulated data were plotted versus time, with the original observed data set and/or percentiles based on the observed data overlaid to visually assess concordance between the model-based simulated data and the observed data.

Final models were used to predict dependent variables (avelumab concentrations and/or ADA data) based on the patients in the data set who were set aside for external validation (20% of the data set) at the individual and population level (the latter using VPCs). These were compared with observations to provide an assessment of the model's predictive ability.

Results

Population PK models with ADA as time-invariant or time-varying covariate on clearance

The increase in avelumab CL attributable to ADA+ status ranged from 8.5% (time-varying model using the time-course of ADA status to influence CL) to 19.9% (time-invariant model with inter-occasion variability [IOV] in CL). The IOV in CL (4%) was negligible compared with inter-individual variability (IIV) in CL (34%), and the inclusion of IOV did not change the estimates of IIV. Simulation-based evaluations (VPCs) confirmed that predictive performance of the PK models was acceptable. The results of the effects of ADA on avelumab CL and the associated computation burden (relative estimation time) are summarized in Table 2. The parameter estimates for each model (Table 7) and the goodness of fit plots for the population PK model (Fig. 9) are provided in the supplementary material.

Table 2 Summary of effect of ADA status on avelumab CL conditioned on the modeling approach

Model Type	Covariate Relationship with TVCL	Time-variant Relationship	Estimated Increase in CL (%) for ADA+	TVCL (L/h)	CL ADA−/CL ADA+ (L/h)	Data Set Modification	Computational Burden*
PPK without IOV in CL							
	None	NA	NA	0.0285	0.0283/0.0332	None	–
	Separate TVCL	No	NA	0.0279/0.335	0.0282/0.0339	None	Low
	ADAEVER	No	19.0	0.0279	0.0282/0.0339	None	Low
	ADAONCE	Yes	10.6	0.0283	0.0282/0.0344	None	Low
	ADALOCF	Yes	8.5	0.0285	0.0293/0.0314	None	Low
	ADALOCF	Yes					
PPK with IOV in CL							
	None	NA	NA	0.0285	0.0289/0.0342	None	High
	ADAEVER	No	19.9	0.0285	0.0280/0.0335	None	High
Joint ADA/PK model							
Mono-directional	Probability of ADA+	Yes	14.9	0.0285 *fix*	0.0261/0.0317	Substantial	High
Bi-directional	Probability of ADA+	Yes	11.6	0.0285 *fix*	0.0258/0.0313	Substantial	High

ADAEVER time-invariant categorical covariate (0 = "ADA− Never" or 1 = "ADA+: At least once"); *ADAONCE* time-variant categorial covariate, *CL* mean of individual clearance values, *IOV* inter-occasion variability (evaluation limited to the first 12 visits), *NA* not applicable, *PPK* population pharmacokinetic, *TVCL* typical population value of clearance

* Computational burden relative to the base model: low: 1–4-fold increase in run times; moderate: 4–8-fold increase in run times; high: > 8-fold increase in run times

Markov models for ADA status

The structures of the population ADA models are provided in Fig. 2 (DTMM), Fig. 3 (CTMM), and Fig. 4 (joint PK-CTMM). In the DTMM, the probability of ADA+ or ADA− status was obtained by estimating the transition probability from ADA status at the current occasion, irrespective of the time since the previous occasion. For the CTMM, the time between occasions was considered to obtain the probability of ADA+ or ADA− status because the influence of the previous ADA status on the probability of the current ADA status typically decreases with increasing time between occasions.

The DTMM estimated the probability of baseline ADA+ status as 2.12% (Table 3). The probability of a transition from ADA− to ADA+ ($p01$) status was 0.7%. The probability of a person transitioning from ADA+ to ADA− status ($p10$) was 25.4%. The relationship between tumor type and $p01$ was the only significant covariate relationship in the model. The estimate of $p01$ was 0.73% for NSCLC (the most common tumor type), 1.8% for GC/GEJC, 0.36% for UC, 0.35% for MCC, and 0% for other solid tumors (including lung, gastrointestinal tract, skin, breast, head and neck cancers). The tumor type relationship with $p01$ in the final SCM model was simplified by removing the relationships between tumor types on $p01$ that were not statistically significant one by one. The relationship between GC/GEJC and $p01$ was the only statistically significant relationship (see Table 3). VPCs confirmed the predictive characteristics of DTMM across tumor types. The VPCs for GC/GEJC tumors are shown in Fig. 5.

The DTMM-predicted time course for ADA+ status ($p1$) was evaluated as a time-varying ADA covariate in the population PK model. This enabled a gradual change to maximal probability when switching from ADA− to ADA+ status instead of an abrupt step change as was the case with the ADAONCE ("Not yet ADA+" or "ADA+ and thereafter") approach (see Fig. 6). The increase in avelumab CL attributable to a transition from ADA− to ADA+ was 41% (90% PI 17%, 52%) in patients with GC/GEJC, 18% (90% PI 18%, 26%) with NSCLC, 11% (90% PI 7%, 12%) with MCC, and 11% (90% PI 7%, 13%) with UC (examples of individual patients are provided in Fig. 6). However, this model did not address the immortal time bias associated with step change from ADA− to ADA+. Although this approach differentiates the effect of ADA+ status on CL between individuals (different maximum probabilities), once an individual's maximum probability is attained, the value remains constant. This approach may be considered a sequential ADA-PK rather than a joint model to link PK and ADA models.

The CTMM estimated the rate of change in ADA status (parameter estimates for the important models are provided in Table 4). The final CTMM included the effects of baseline ADA status and tumor type on the rate constant for changing from ADA− to ADA+ (λ_{01}). This rate constant was 3.8-fold higher when patients were ADA+ at baseline. Compared to NSCLC, λ_{01} was 17% higher in patients with GC/GEJC, 37% lower with UC, 38% lower

Table 3 NONMEM parameter estimates for the discrete-time Markov models

Parameter	Base Model		Final SCM model		Reduced Covariate Model	
DTMM model		%RSE		%RSE		%RSE
OFV	2517.934		2479.973		2485.735	
ΔOFV	0		− 37.961		− 32.199	
Typical value for P1 at baseline (logit scale)	− 3.83	1.3%	− 3.83	1.6%	− 3.83	1.1%
Typical value for P01 (logit scale)	− 4.93	4.2%	− 4.91	4.5%	− 5.05	4.5%
Typical value for P10 (logit scale)	− 1.08	6.2%	− 1.08	9.7%	− 1.08	5.2%
Change in P01 relative to NSCLC						
GC/GEJC			− 0.191	22.4%	− 0.215	17.1%
UC			0.142	68%		
MCC			0.157	67.5%		
Other solid tumors			0.971	71.9%		
IIV on P1 baseline, %	7.1%*		7.1%*		7.1%*	
IIV on P01, %	186.6%	15.7%	132.1%	31.8%	129.1%	27.9%
IIV on P10, %	7.1%*		7.1%*		7.1%*	

OFV objective function value, *ΔOFV* change in OFV from baseline model, *P1* probability of ADA+, *P01* probability to transition from ADA− to ADA+, *P10* probability to transition from ADA+ to ADA−, *%RSE* relative standard error (percentage), *SCM* stepwise covariate model

*Indicates fixed parameters

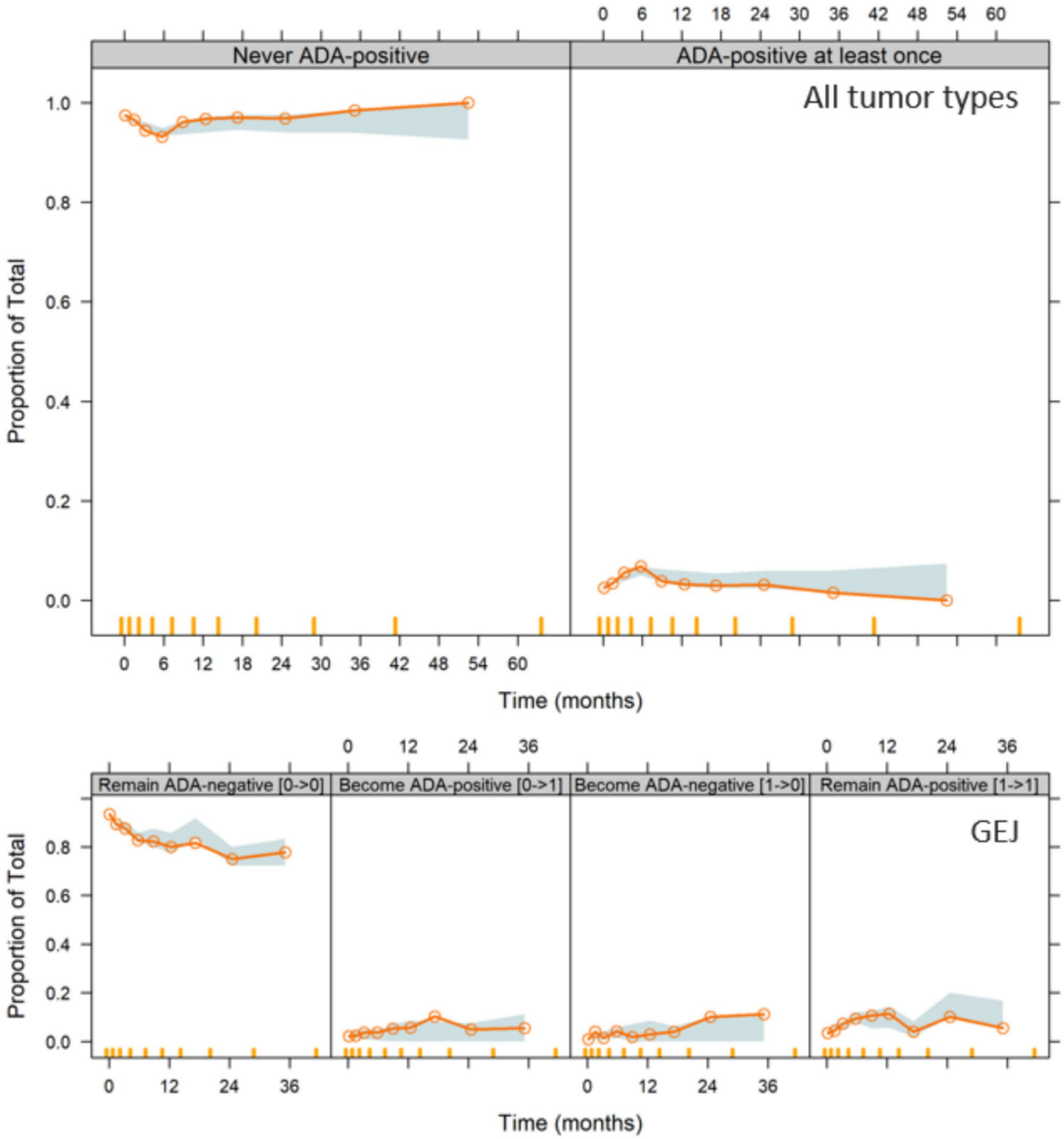

Fig. 5 Visual predictive check for the population discrete-time Markov model. Top panel: all tumor types. Bottom panel: GC/GEJC tumors (in JAVELIN Gastric 100). The open circles show the observed fractions versus time and the shaded area shows the corresponding model-based 95% confidence interval

with MCC, and 99% lower with other solid tumors (there were no ADA+ patients in the model development data set). The model under-predicted the time-course of the probability of ADA status for the patients with NSCLC in the later part of study JAVELIN Lung 100. The final CTMM included the same covariate relationships as in the final DTMM: baseline ADA status and tumor type on λ_{01}. The VPCs for the final model are shown in Fig. 7.

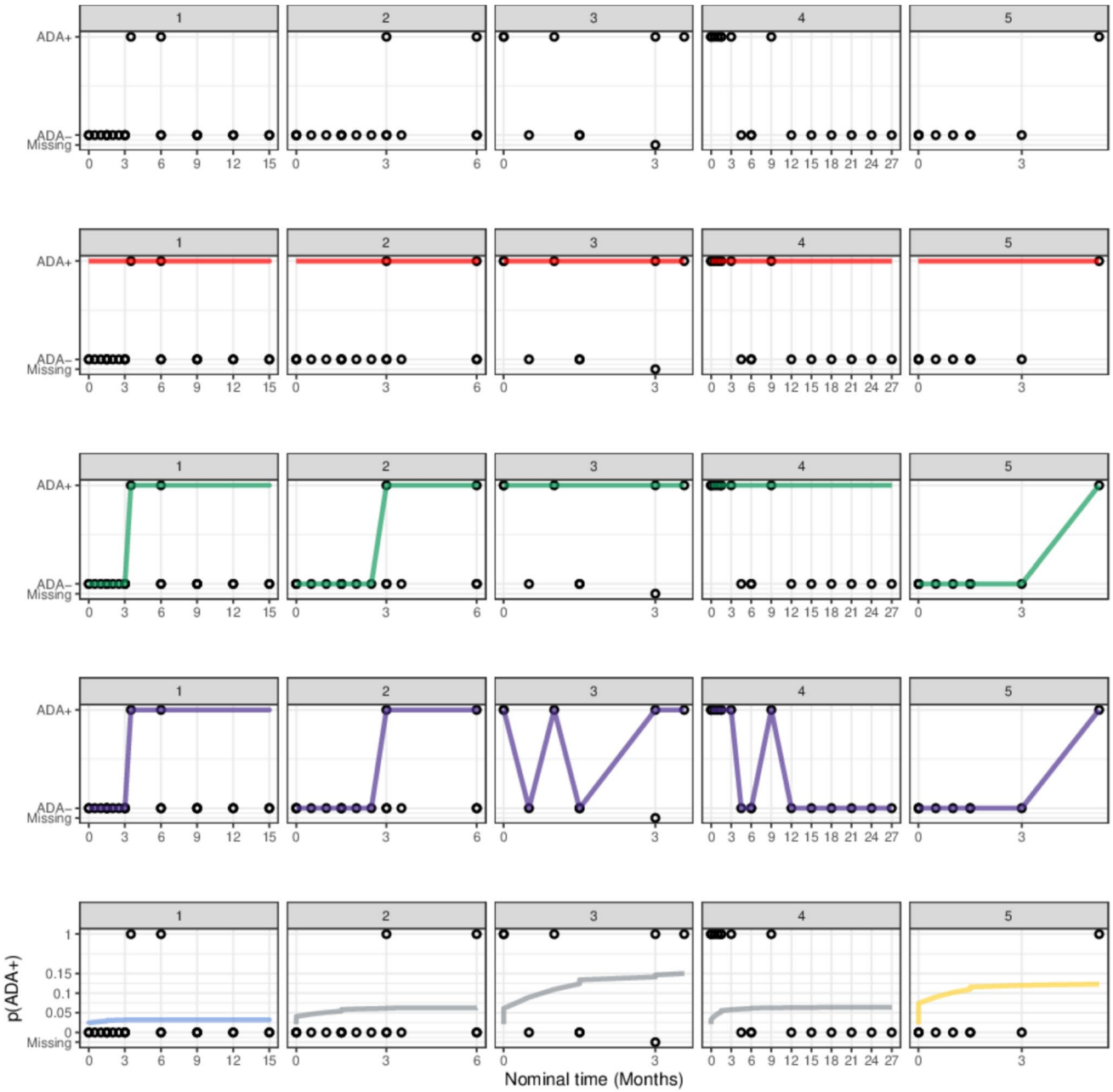

Fig. 6 Demonstration of the time-course of probability of ADA+ and the time-invariant (ADAEVER) and time-variant (ADAONCE, ADALOCF) categorization of the ADA data for five random patients who were ADA+ at least once. The open circles show the actual ADA values. The red lines show the values for ADAEVER, the green lines are ADAONCE, and the purple lines are ADALOCF. The light blue line is MCC, gray lines are NSCLC, and the yellow line is GC/GEJC. p(ADA+) is the individual probability of ADA+ from the discrete time Markov model

Joint PK-ADA models

The parameter estimates for the important models are provided in Table 5. The time-course of $p1$ compared to other ADA categorizations for several randomly selected patients is shown in Fig. 8.

The relationship between $p1$ and CL was estimated, and the maximum increase in clearance was 11.6% and 15.0% for the mono- and bi-directional joint PK-ADA models for the linear model and 21.7% for the nonlinear model, respectively. With respect to the relationship between avelumab exposure and λ_{01}, maximum decrease in λ_{01} was 37% with

Table 4 NONMEM parameter estimates continuous-time Markov model

Parameter						
CTMM Model	Base Model	%RSE	Baseline ADA+ on λ_{01}	%RSE	Final Model	%RSE
OFV	5452566.033		5452534.992		5452478.918	
ΔOFV	0		− 31.041		− 87.115	
Typical value for λ_{01}, /h	0.00461	18.10%	0.00446	18.10%	0.00404	20.50%
Typical value for λ_{10}, /h	0.139	17.60%	0.142	17.80%	0.146	17.70%
Baseline ADA+: change in λ_{01}			4.84	40.50%	4.38	42.20%
Change in λ_{01} relative to NSCLC						
GC/GEJC					1.17	30%
UC					− 0.404	48%
MCC					− 0.373	88.50%
Other solid tumors					− 0.99*	
IIV on λ_{01}, %	0%*		0%*		0%*	
IIV on K21, %	0%*		0%*		0%*	

OFV objective function value, *ΔOFV* change in OFV from baseline model, λ_{01} transit rate constant ADA− to ADA+, λ_{10} transit rate constant ADA+ to ADA−, *%RSE* relative standard error (percentage)

*Indicates fixed parameters

50% of the maximum decrease estimated to occur at a concentration of 349 µg/mL. This estimate is markedly higher than the maximum avelumab concentration for adults for the clinical dose 800 mg q2w (geometric mean 256.3 µg/mL [24]). The relationship curve was relatively steep with γ of 2.58.

The portion of the data set not used in the model development was reserved for external validation. VPCs were performed with the parameter estimates from the model development data set. The VPCs confirmed that the PK models with ADA status as a time-varying covariate, the final DTMM, and final CTMM were all able to predict the new data with acceptable accuracy and confirmed the predictive ability of the models.

Discussion

Joint models refer to models that simultaneously analyze different types of outcomes or variables [25]. Bi-directional joint models are models that consider interactions of relationships in both directions between the outcomes or variables. Broadly speaking, joint modeling is the estimation of two or more statistical submodels into a single joint model. Such models provide more efficient estimates of the effects and can reduce bias in the estimates of the overall effect [26].

We developed a joint model to describe the bi-directional effects of the probability of ADA+ status (a CTMM) on the CL of avelumab (a two-compartment disposition PK model with time-varying clearance) and the effect of the avelumab concentrations on the rate of ADA− to ADA+ transition. In this analysis both the PK and ADA models were described using ODEs, which facilitated combining the ADA and PK models. The ADA and PK models were linked by estimating the correlation in the random effects (inter-individual variability) in clearance (CL) and transition rate constant (λ_{01}) and by separate link functions for the effect of ADA+ on CL (a sigmoidal Emax model) and the effect of the amount of avelumab in the central compartment on λ_{01}. Insufficient data were available to assess the impact of neutralizing antibodies.

Joint models are computationally intensive. A stepwise approach was used, starting with the development of separate PK and ADA models, with the models with shorter runtimes explored first (population PK model without IOV, and DTMM of ADA) before developing the models that required longer (the CTMM for ADA, and the joint CTMM ADA-PK model). Both the PK and ADA CTMM were modeled using sets of ODEs, resulting in long runtimes, but this made subsequent combination of the models more straightforward (see Fig. 4).

Effect of ADA on avelumab CL was previously estimated (using ADAEVER) as 12.3% (95% CI 7%, 18%) in a full covariate model [11]. For the current analysis, the model was reduced to the base model with bodyweight as the only maintained covariate. With the reduced model the ADA effect on clearance ranged from 8.5% (ADALOCF) to 19.9% (ADAEVER with IOV in CL). The estimates of IIV on clearance or the estimates of the parameters describing the time-varying component of clearance did not appear to be influenced by different ADA categorizations.

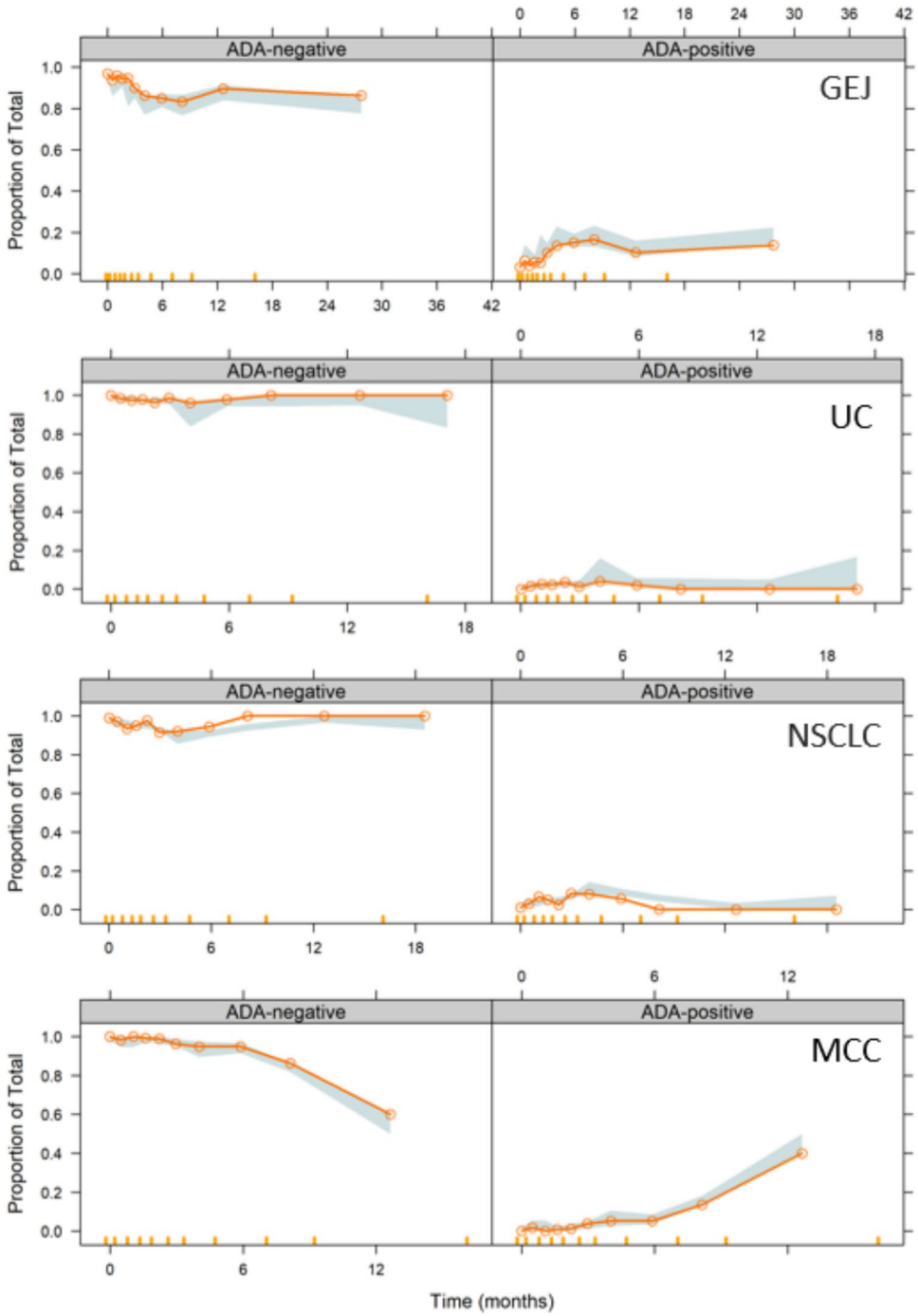

Fig. 7 Visual predictive check for the final continuous-time Markov model for GC/GEJC, UC, NSCLC, and MCC. The open circles show the observed fractions versus time and the shaded area shows the corresponding model-based 95% confidence interval

Modeling immunogenicity has been approached in a number of ways in the literature, most commonly by incorporating as a binary variable on CL in the covariate submodel [27, 28]. Several alternative approaches have been proposed at scientific meetings, but few have been published in peer-reviewed form to date. One suggested approach, which addressed interspecies scaling of a recombinant complement factor I, used a mixture model with two populations representing the presence and absence of ADA-dependent clearance in non-human primates, and included estimation of an ADA-dependent CL and an additional CL parameter along with the time of its onset to account for the potential effects of ADA in humans [29]. A more complex approach proposed by Niebecker et al. comprised modeling immune response (time of seroconversion) using an ADA surrogate [28]. In another approach, a semi-mechanistic PK/PD model was developed to characterize the dynamics of ADA in cancer patients receiving the V937 oncolytic virus

Table 5 NONMEM parameter estimates joint PK and ADA models

Parameter					
Joint Model	Base Model	Correlation CL, C1, λ_{01}	ADA on CL	ADA on CL + C1 on ADA	ADA on CL (Emax) + C1 on ADA
OFV	20230779.285	20230699.696	20230703.331	20230659.164	20230709.255
ΔOFV	0	− 79.589	− 75.954	− 120.121	− 70.03
Avelumab population PK model					
Clearance (CL), L/h	0.0272*	0.028	0.0272*	0.0275	0.0272*
Central volume (V1), L	3.52*	3.52*	3.52*	3.52*	3.52*
Peripheral volume, L	0.582*	0.582*	0.582*	0.582*	0.582*
Intercompartmental clearance, L/h	0.0128*	0.0128*	0.0128*	0.0128*	0.0128*
I_{max}	− 0.015*	− 0.015*	− 0.015*	− 0.015*	− 0.015*
T_{50}, days	51.9*	51.9*	51.9*	51.9*	51.9*
γ	2.59*	2.59*	2.59*	2.59*	2.59*
Continuous Markov model					
Rate constant ADA− to ADA+ (λ_{01}), /h	0.00404*	0.00404	0.00404*	0.00406	0.00404*
Rate constant ADA+ to ADA− (λ_{10}), /h	0.146*	0.146*	0.146*	0.146*	0.146*
Change in λ_{01} relative to NSCLC					
GC/GEJC	1.17*	1.17*	1.17*	1.17*	1.17*
UC	− 0.404*	− 0.404*	− 0.404*	− 0.404*	− 0.404*
MCC	− 0.373*	− 0.373*	− 0.373*	− 0.373*	− 0.373*
Other solid tumors	− 0.99*	− 0.99*	− 0.99*	− 0.99*	− 0.99*
Baseline ADA+: change in K34	4.38*	4.38*	4.38*	4.38*	4.38*
Effect of ADA on CL					
Slope of ADA effect on CL			0.116	0.15	
Maximum change					0.217
50% of maximum change					0.446
Shape of effect curve					1
Effect of exposure on ADA					
Maximum change				− 0.374	− 0.405
50% of maximum change				349	387
Shape of effect curve				2.58	2.75
IIV on CL, %	38.5%	40.1%	38.5%	39.9%	46.1%
IIV on V1, %	23.4%	25.7%	23.4%	24.6%	24.8%
IIV on λ_{01}, %	218.1%	226.1%	218.1%	329%	414.4%
IIV on λ_{10}, %	0%*	0%	0%*	0%	0%
IIV on TMAX, %	21.8%*	21.8%*	21.8%*	21.8%*	21.8%*
Proportional residual error PK (σ_{prop}), %	21.1%*	21.1%*	21.1%*	21.1%*	21.1%*
Additive residual error PK (σ_{add}), ng/mL	2378.6*	2378.6*	2378.6*	2378.6*	2378.6*

CL clearance, *C1* avelumab concentration in central compartment, *OFV* objective function value, *ΔOFV* change in OFV from baseline model, λ_{01} transit rate constant ADA− to ADA+, λ_{10} transit rate constant ADA+ to ADA−, γ^{P1} shape of the effect curve for ADA on CL; γ^{C1}: shape of the effect curve for exposure on ADA

*Indicates fixed parameters

in monotherapy or in combination with pembrolizumab, whereby the time course of ADA was modeled using the population-pharmacokinetic parameter-and data (PPP&D) approach [30], in which population PK parameters are fixed, but individual PK parameters are estimated simultaneously with the ADA model based on both PK and ADA data [31]. Time to event models have also been employed to describe the time to appearance of ADA [27]. Therein,

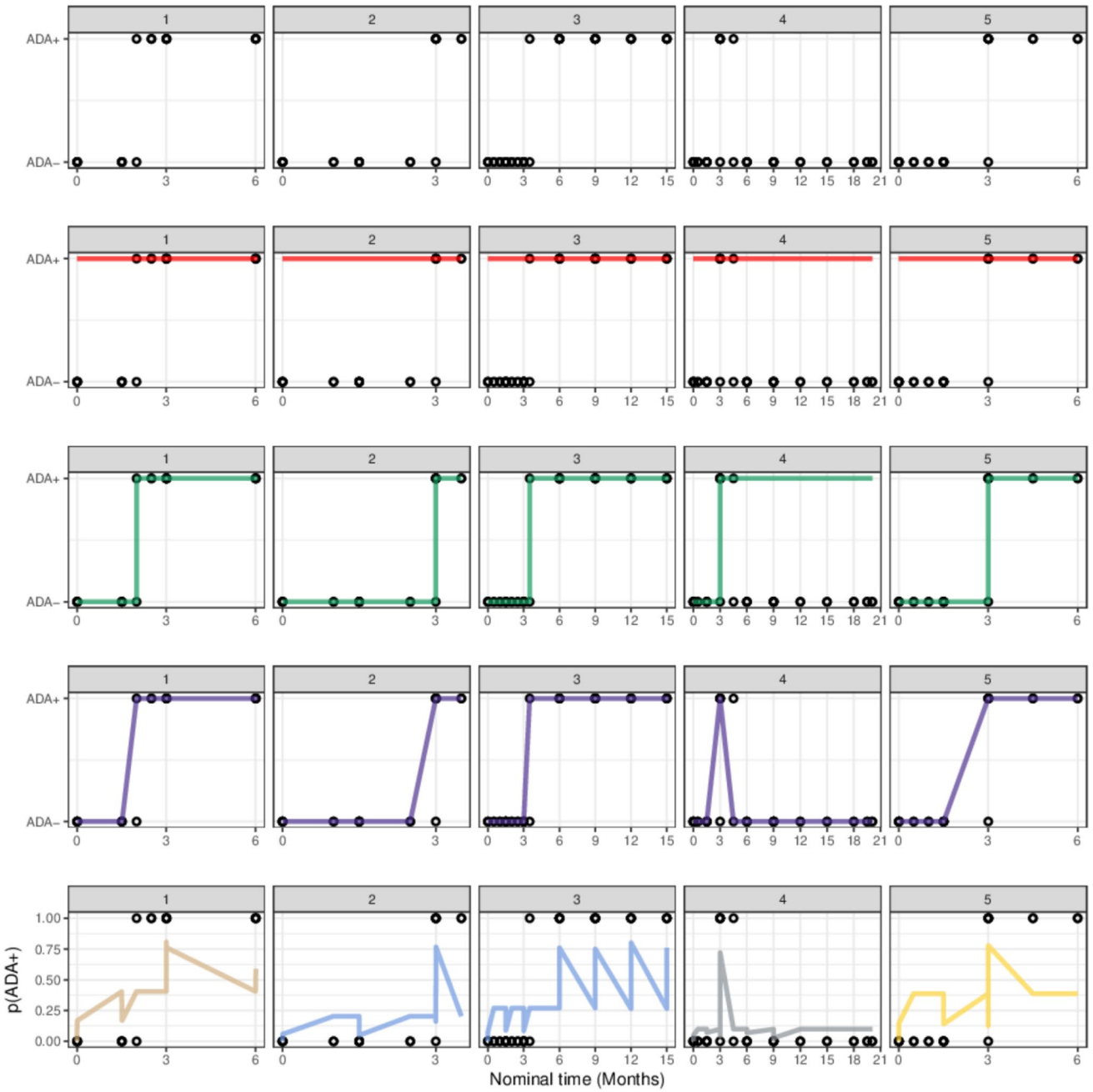

Fig. 8 Demonstration of the time-course of probability of ADA+ [p(ADA+)] and the time-invariant (ADAEVER) and time-variant (ADAONCE, ADALOCF) categorization of the ADA data for five random patients who were ADA+ at least once. The open circles show the actual ADA values. The lines show the values for ADAEVER, the solid green lines are ADAONCE, and the purple dotted lines are ADALOCF. The light blue line is MCC, gray lines are NSCLC, and the yellow line is GC/GEJC

ADA formation, which mainly took place within 3 months of starting the treatment, was predicted to be lower with higher trough concentrations, which could be achieved with the use of higher doses and/or increased dosing frequency (e.g. loading doses) [32].

In immuno-oncology settings, during treatment with immune checkpoint inhibitors including avelumab, time-variance in CL, attributed to changes in disease status, has been observed [11, 32, 33]. Consequently, exposure–response analyses using baseline exposure metrics have been found to be more consistent with the true exposure/dose–response relationship. The use of time-invariant ADA (ADAEVER) as a binary covariate may affect the estimate of baseline CL and derived exposure metrics that may mask or confound the true exposure–response relationship. Additionally, due to the fact that the ADAEVER approach conservatively treats all

Table 6 Considerations and utility of the population PK, ADA, and joint PK-ADA models

Model	Considerations	Utility
Population PK with IOV in clearance	The clinical relevance of the ADA effect on PK may not yet be fully characterized in early phases of clinical drug development. However, the assessment of IOV to gauge changes in variability in clearance (not specifically related to ADA) over time could be performed with data from well-controlled phase 1/2 studies in which rich PK are collected (compared with sparse PK data in phase 3/confirmatory trials). Depending on the complexity of the population PK model, the large number of occasions (study visits) in longer trials may prohibit the use of the IOV model for covariate evaluations due to high computational burden	Evaluation of the parameters (random effects) associated with IOV at each occasion may indicate trends in PK parameters (clearance) with time that could be attributable to ADA effects Evaluation of changes in time-dependent PK parameters when IOV is included, and potential confounding when estimating ADA-PK relationships Exploratory (graphical) analysis of the random effect values to evaluate potential covariate relationships (e.g. tumor type)
Population PK with IOV and ADA covariate relationships	Maintain IOV in the model if computationally feasible and/or clinically important (e.g. narrow therapeutic window) Assess ADA relationship with important PK parameters (clearance) If ADA status is related to adverse events, time-varying models should be considered for longitudinal assessment of safety	Estimate the magnitude of the ADA effect on PK (and drug exposure) to assess clinical importance (in conjunction with other clinical considerations) Re-evaluate time-dependent PK when ADA effects are added to the model, including differences between tumor types (or other important covariates from the graphical analyses)
DTMM	DTMM typically has few fixed effects and no or limited random effects with relatively fast run times. Due to the low computational burden DTMM are ideal for a broad covariate evaluation (e.g. SCM) Limited changes to the data set are required if time-varying ADA data are included in the population PK data set (use ADA as DV column). Prior ADA status can be added to the data set or obtained on the run in the model control stream Output of the individual time-course of ADA+ probability ($p1$) may be added to the data set for a sequential DTMM-PK model. Time-varying ADA data are usually binary (values of 0 or 1) with a step change; the DTMM provide a gradual change in ADA status with individual maximal values (range 0–1)	Obtain population estimates for probability of ADA+ status, including at baseline Covariate relationships are not time-consuming and may be thoroughly assessed using automated search strategies Covariate relationships may be included in the evaluation of the ADA as a time-varying covariate in the population PK model using a sequential DTMM-PK model Covariate relationships for DTMM will facilitate the covariate model development/evaluation for CTMM that may be limited owing to the latter's high computational burden
CTMM	Due to the high computational burden, especially with large data sets, CTMM development could start with the most informative data set (e.g. limited to the study or tumor type with the highest quantity/quality of ADA data) Substantial changes to the data set are required for implementation in NONMEM. The Markovian elements (prior ADA status) are incorporated as compartment amounts that are set to 1 (100% probability) or 0 (0% probability) using the associated bioavailability parameter Long run times may limit covariate model development but may be informed by the results of a prior DTMM covariate evaluation Random effects may not be estimable or may lack adequate precision, which may impact the development of a joint PK-ADA model (see Joint PK-ADA recommendations below)	CTMM may be more appropriate for non-uniform observation times. However, ADA data are collected at uniform times in clinical trials, and DTMM and CTMM methods produce similar results Reserve CTMM development for small data sets or in scenarios in which ADA data will be jointly analyzed with non-uniform data (e.g. adverse event data)

Table 6 (continued)

Model	Considerations	Utility
Joint PK-ADA	Assess correlations in the PK and ADA model parameters (clearance and ADA transition rates) prior to combining the PK and ADA models in a joint model to assess feasibility for developing a joint model If the population PK model is coded using sets of differential equations, combination with CTMM is feasible. As a first step the correlation in clearance and the transition rate from ADA− to ADA+ should be estimated. If the CTMM did not include IIV in transition rates, assign the estimate from the DTMM as the initial estimate or fix IIV to a large value (e.g. 2)	The joint model may be helpful to understand differences in efficacy and/or safety profiles with dose adjustments in different studies, prior treatment experiences, or with unexpected clinical findings. This approach also enables simulations of alternate dosing regimens with respect to the probability/time-course of ADA development Robust, stable population PK models and CTMM should be developed prior to developing the joint models. The computational burden will limit the number of parameters that may be estimated (depending on the size of the data set) Depending on the complexity of the bi-directional effects, longitudinal models may be useful to answer questions relating to the effects of exposure on probability of becoming ADA+: - concentrations in which the probability may exceed a specific threshold (e.g. 50%) and to relate this point to concentration ranges for specific tumor types, or concentrations of interest (e.g. Cmax or trough concentrations); - the impact of increasing concentrations of drug on the probability of becoming ADA+; - the probability of becoming ADA+ at time-points of interest to simplify the protocol requirements for ADA data collection

time points during treatment as being ADA+, bias is introduced in estimation of the effect of immunogenicity on CL, questioning the accuracy of estimates of ADA effect on PK. The estimated time to reach 50% of the maximum change in CL was consistent for all ADA covariate models (around 12 months after starting treatment). During this period the DTMM demonstrated that the probability of remaining ADA− decreased rapidly (Fig. 5), again demonstrating the importance of unbiased estimates of baseline CL for exposure–response analyses. The estimation of IOV in a large data set with a long period of observation is cumbersome and drastically increases the computational burden (Table 2), as well as introducing significant additional complexity when using models for simulation. Assessment of IOV should be performed early during the development program to ensure that the clinical importance of the observed heterogeneity in the mechanisms and outcomes is understood prior to analyzing data from pooled studies or studies with long duration. In this analysis, the IOV over the first 12 visits was investigated, due to the large number of visits in study JAVELIN Lung 100. The first 12 visits covered a period of ca. 3 years (168 weeks, range 148 to 198 weeks) and provided adequate coverage of the observed ADA transitions. The addition of IOV in CL did not change the estimate of the ADA effect on CL: across the models the increase in CL due to ADA using a time-invariant covariant was 20%. The estimate of IOV in CL was 4% across all models and thus negligible compared to the estimate of IIV in CL of 34%. Thus, IOV was not incorporated in the final joint PK-ADA models.

Markov models have previously been used to analyze ADA dynamics. Hidden Markov (HM) models were developed for satralizumab, a humanized IgG2 monoclonal recycling IL-6 receptor antagonist for treatment of neuromyelitis [34], and certolizumab pegol, a PEGylated Fc-free TNF inhibitor for treatment of chronic inflammatory diseases [35]. A HM model is a class of probabilistic models that connect observable variables (e.g. ADA+ or ADA−) to hidden underlying states (immunological response) where the next state depends on the previous state [34]. The probabilities of the observed ADA-state to the hidden immunological state were modeled as continuous random variables that could be correlated through a bivariate Gaussian probability density function [35]. The HM ADA models assumed that all patients started in a state of no ADA production, and only the probabilities of transition were estimated. The stationary probabilities (ADA− transition to ADA−, and ADA+ transition to ADA+) were not estimated. The HM model for certolizumab pegol suggested that ADA are formed earlier than assays can detect. In the analysis of ADA data for avelumab, DTMM estimated that 2.2% of patients were positive at baseline, and baseline ADA+ status was a covariate in the DTMM and CTMM

models. Although this estimate is in agreement with the incidence of positive baseline ADAs in clinical trials (range 1% to 20%) [36], the covariate was estimated with high uncertainty in the CTMM, indicating that caution is needed when interpreting transition rates in patients with positive baseline ADA measurements. As estimating the stationary probability (ADA+ transition to ADA+) was required, the HM model as implemented for certolizumab pegol was not considered appropriate for the current analysis.

In the DTMM, the probability of a transition from ADA− to ADA+ ($p01$) status was 0.7% whereas the probability of a patient transitioning from ADA+ to ADA− status ($p10$) was 25.4%. This difference may reflect the natural decline in antibody levels due to a diminished immune response or immune tolerance, treatment interventions (such as immunosuppressive therapies), or variability in sensitivity and specificity in assays used to detect ADA [37].

The bidirectional joint PK-ADA model we developed for avelumab suggested that higher avelumab concentrations resulted in a decrease in transition rate to the ADA+ state. This finding is in line with the previous analyses [30, 38], including application of HM models, which have indeed proposed that increased drug exposure reduces immunogenicity, although such findings in oncology are somewhat conflicting [38]. Differences in ADA rates among tumor types have previously been reported for another immune checkpoint inhibitor, pembrolizumab, although the ADA incidence was overall low [39]. In addition, there was high uncertainty in the estimates of the differences between tumor types (%RSE > 30%), indicating that the data set did not contain adequate information and should be interpreted with caution. A pooled analysis of 12 atezolizumab clinical trials did not identify meaningful differences in ADA incidence between tumor types [40].

We have proposed considerations and utility of the population PK, ADA, and joint PK-ADA models (Table 6). There is a fine balance between the information gained and resources required to do so. All three approaches were successful in providing quantitative insight into the relationship between avelumab exposure and ADA formation. Accounting for the phase of development, data available, and clinical need to understand the relationship between ADA dynamics and drug exposure, efficacy and/or safety can help guide the choice of the type of analysis most appropriate.

Conclusions

This analysis investigated approaches to quantitatively account for immunogenicity in an immuno-oncology setting for an immune checkpoint inhibitory monoclonal antibody. The approaches included ADA as a covariate in a population PK model and Markov models of ADA status (ADA+ or ADA−). The final joint PK-ADA model incorporated bidirectional effects of ADA status on avelumab clearance and avelumab exposure on ADA status. None of the investigated covariates other than baseline ADA status and tumor type were of relevance for assessing avelumab immunogenicity. The joint PK-ADA model estimated a lower rate of change from ADA− to ADA+ status with higher avelumab concentrations. Viewed from a broader perspective, the analyses presented here illustrate a roadmap for approaching quantitative characterization of the interrelationships of dynamics of PK and ADA for quantitative clinical pharmacology characterization of biologics.

Supplementary Information The online version contains supplementary material available at https://doi.org/10.1007/s10928-025-09971-w.

Author contribution J.S.W., J.W. and A.-M.M.-G. wrote the manuscript. A.K., A.-M.M.-G., J.W., J.S.W. and K.V. designed the research. J.S.W. and J.W. performed the research. All authors analyzed the data. All authors reviewed and approved the final manuscript.

Funding The study was sponsored by the healthcare business of Merck KGaA, Darmstadt, Germany (CrossRef Funder ID: 10.13039/100009945).

Data availability Any requests for data by qualified scientific and medical researchers for legitimate research purposes will be subject to the healthcare business of Merck KGaA, Darmstadt, Germany's (CrossRef Funder ID: 10.13039/100009945) Data Sharing Policy. All requests should be submitted in writing to the healthcare business of Merck KGaA, Darmstadt, Germany's data sharing portal (https://www.emdgroup.com/en/research/our-approach-to-research-and-development/healthcare/clinical-trials/commitment-responsible-data-sharing.html). When the healthcare business of Merck KGaA, Darmstadt, Germany has a co-research, co-development, or co-marketing or co-promotion agreement, or when the product has been out-licensed, the responsibility for disclosure might be dependent on the agreement between parties. Under these circumstances, the healthcare business of Merck KGaA, Darmstadt, Germany will endeavor to gain agreement to share data in response to requests.

Declarations

Conflict of interest JSvdW and JJW were employed as consultants by Merck KGaA when analyses were performed. AK was an employee of the healthcare business of Merck KGaA, Darmstadt, Germany at time of the analysis. KV is an employee of EMD Serono, Billerica, MA, USA. WG was an employee of EMD Serono, Billerica, MA, USA at time of the analysis. AMM is an employee of the healthcare business of Merck KGaA, Darmstadt, Germany.

References

1. Swanson SJ (2006) Immunogenicity issues in drug development. J Immunotoxicol 3(3):165–172. https://doi.org/10.1080/15476910600908852
2. Enrico D, Paci A, Chaput N, Karamouza E, Besse B (2020) Antidrug antibodies against immune checkpoint blockers: impairment of drug efficacy or indication of immune activation? Clin Cancer Res 26(4):787–792. https://doi.org/10.1158/1078-0432.CCR-19-2337
3. Jani M, Barton A, Warren RB, Griffiths CE, Chinoy H (2014) The role of DMARDs in reducing the immunogenicity of TNF inhibitors in chronic inflammatory diseases. Rheumatology (Oxford) 53(2):213–222. https://doi.org/10.1093/rheumatology/ket260
4. Fernandez L, Bustos RH, Zapata C, Garcia J, Jauregui E, Ashraf GM (2018) Immunogenicity in protein and peptide based-therapeutics: an overview. Curr Protein Pept Sci 19(10):958–971. https://doi.org/10.2174/1389203718666170828123449
5. Tatarewicz SM, Mytych DT, Manning MS, Swanson SJ, Moxness MS, Chirmule N (2014) Strategic characterization of anti-drug antibody responses for the assessment of clinical relevance and impact. Bioanalysis 6(11):1509–1523. https://doi.org/10.4155/bio.14.114
6. Khandelwal A, Grisic AM, French J, Venkatakrishnan K (2022) Pharmacometrics golems: exposure-response models in oncology. Clin Pharmacol Ther 112(5):941–945. https://doi.org/10.1002/cpt.2564
7. Bajaj G, Suryawanshi S, Roy A, Gupta M (2019) Evaluation of covariate effects on pharmacokinetics of monoclonal antibodies in oncology. Br J Clin Pharmacol 85(9):2045–2058. https://doi.org/10.1111/bcp.13996
8. Collins JM, Gulley JL (2019) Product review: avelumab, an anti-PD-L1 antibody. Hum Vaccin Immunother 15(4):891–908. https://doi.org/10.1080/21645515.2018.1551671
9. Bavencio (avelumab) 2024 Summary of product characteristics. Merck Europe B.V., Amsterdam, Netherlands, an affiliate of Merck KGaA.
10. Ooi QX, Plan E, Bergstrand M (2025) A tutorial on pharmacometric Markov models. CPT Pharmacometrics Syst Pharmacol 14(2):197–216. https://doi.org/10.1002/psp4.13278
11. Wilkins JJ, Brockhaus B, Dai H, Vugmeyster Y, White JT, Brar S, Bello CL, Neuteboom B, Wade JR, Girard P, Khandelwal A (2019) Time-varying clearance and impact of disease state on the pharmacokinetics of avelumab in Merkel cell carcinoma and urothelial carcinoma. CPT Pharmacometrics Syst Pharmacol 8(6):415–427. https://doi.org/10.1002/psp4.12406
12. Hu P, Dai HI, Bourdage J, Zhou D, Trang K, Kowalski K, Bello C, Hibma J, Khandelwal A, Cowan K, Dong J, Venkatakrishnan K, Gao W (2024) Immunogenicity of avelumab in patients with metastatic Merkel cell carcinoma or advanced urothelial carcinoma. Clin Transl Sci 17(3):e13730. https://doi.org/10.1111/cts.13730
13. Liu C, Yu J, Li H, Liu J, Xu Y, Song P, Liu Q, Zhao H, Xu J, Maher VE, Booth BP, Kim G, Rahman A, Wang Y (2017) Association of time-varying clearance of nivolumab with disease dynamics and its implications on exposure response analysis. Clin Pharmacol Ther 101(5):657–666. https://doi.org/10.1002/cpt.656
14. Anderson BJ, Holford NH (2008) Mechanism-based concepts of size and maturity in pharmacokinetics. Annu Rev Pharmacol Toxicol 48:303–332. https://doi.org/10.1146/annurev.pharmtox.48.113006.094708
15. Karlsson MO, Schoemaker RC, Kemp B, Cohen AF, van Gerven JM, Tuk B, Peck CC, Danhof M (2000) A pharmacodynamic Markov mixed-effects model for the effect of temazepam on sleep. Clin Pharmacol Ther 68(2):175–188. https://doi.org/10.1067/mcp.2000.108669
16. Snelder N, Diack C, Benson N, Ploeger B (2009) Towards the implementation of the Markov property into a continuous-time transition state model in NONMEM. PAGE. 18: 1536
17. Bergstrand M, Soderlind E, Weitschies W, Karlsson MO (2009) Mechanistic modeling of a magnetic marker monitoring study linking gastrointestinal tablet transit, in vivo drug release, and pharmacokinetics. Clin Pharmacol Ther 86(1):77–83. https://doi.org/10.1038/clpt.2009.43
18. Karlsson M (2012) Introduction to Markov modelling. PAGE. 21: 2636
19. Beal SL, Sheiner LB, Boeckmann AJ, Bauer RJ (2016) NONMEM Users' Guides. Ellicott City, Maryland, USA: ICON Development Solutions.
20. Savic RM, Karlsson MO (2009) Importance of shrinkage in empirical Bayes estimates for diagnostics: problems and solutions. AAPS J 11(3):558–569. https://doi.org/10.1208/s12248-009-9133-0
21. Lindbom L, Ribbing J, Jonsson EN (2004) Perl-speaks-NONMEM (PsN)–a Perl module for NONMEM related programming. Comput Methods Programs Biomed 75(2):85–94. https://doi.org/10.1016/j.cmpb.2003.11.003
22. Lindbom L, Pihlgren P, Jonsson EN (2005) PsN-Toolkit–a collection of computer intensive statistical methods for non-linear mixed effect modeling using NONMEM. Comput Methods Programs Biomed 79(3):241–257. https://doi.org/10.1016/j.cmpb.2005.04.005
23. Jonsson EN, Nyberg J (2022) A quantitative approach to the choice of number of samples for percentile estimation in bootstrap and visual predictive check analyses. CPT Pharmacometrics Syst Pharmacol 11(6):673–686. https://doi.org/10.1002/psp4.12790
24. Vugmeyster Y, Grisic AM, Brockhaus B, Rueckert P, Ruisi M, Dai H, Khandelwal A (2022) Avelumab dose selection for clinical studies in pediatric patients with solid tumors. Clin Pharmacokinet 61(7):985–995. https://doi.org/10.1007/s40262-022-01111-8
25. Lawrence Gould A, Boye ME, Crowther MJ, Ibrahim JG, Quartey G, Micallef S, Bois FY (2015) Joint modeling of survival and longitudinal non-survival data: current methods and issues. Report of the DIA Bayesian joint modeling working group. Stat Med. 34 (14): 2181–2195. https://doi.org/10.1002/sim.6141
26. Hickey GL, Philipson P, Jorgensen A, Kolamunnage-Dona R (2016) Joint modelling of time-to-event and multivariate longitudinal outcomes: recent developments and issues. BMC Med Res Methodol 16(1):117. https://doi.org/10.1186/s12874-016-0212-5
27. Dirks NL, Meibohm B (2010) Population pharmacokinetics of therapeutic monoclonal antibodies. Clin Pharmacokinet 49(10):633–659. https://doi.org/10.2165/11535960-000000000-00000
28. Niebecker R, Kloft C (2012) Modelling of anti-drug antibodies directed against a monoclonal antibody. PAGE. 21: 2432
29. Ayoun Alsoud R, Le Moan N, Holten-Andersen L, Knudsen T, Lennernas H, Simonsson USH (2024) Model-based interspecies scaling for predicting human pharmacokinetics of CB 4332, a

complement factor I protein. J Pharm Sci 113(9):2895–2903. https://doi.org/10.1016/j.xphs.2024.06.022
30. Zhang L, Beal SL, Sheiner LB (2003) Simultaneous vs sequential analysis for population PK/PD data I: best-case performance. J Pharmacokinet Pharmacodyn 30(6):387–404. https://doi.org/10.1023/b:jopa.0000012998.04442.1f
31. Parra-Guillen ZP, Trocóniz IF, Freshwater T (2023) Modeling the dynamics of anti-drug antibodies in cancer patients treated with oncolytic virus in monotherapy or in combination with immune check- point inhibitors. PAGE 31: 10687
32. Lacroix BD, Kirby H, Oliver R, Parker G, Friberg LE, Karlsson MO (2015) A time-to-event model for the immunogenicity of certolizumab pegol in rheumatoid arthritis subjects. PAGE 24: 3554
33. Dai HI, Vugmeyster Y, Mangal N (2020) Characterizing exposure-response relationship for therapeutic monoclonal antibodies in immuno-oncology and beyond: challenges, perspectives, and prospects. Clin Pharmacol Ther 108(6):1156–1170. https://doi.org/10.1002/cpt.1953
34. Leisegang R, Silber Baumann HE, Lennon-Chrimes S, Ito H, Miya K, Genin JC, Plan EL (2024) Immunogenicity dynamics and covariate effects after satralizumab administration predicted with a hidden Markov model. CPT Pharmacometrics Syst Pharmacol 13(12):2171–2184. https://doi.org/10.1002/psp4.13230
35. Brekkan A, Lledo-Garcia R, Lacroix B, Jonsson S, Karlsson MO, Plan EL (2024) Characterization of anti-drug antibody dynamics using a bivariate mixed hidden-Markov model by nonlinear-mixed effects approach. J Pharmacokinet Pharmacodyn 51(1):65–75. https://doi.org/10.1007/s10928-023-09890-8
36. Usdin M, Quarmby V, Zanghi J, Bernaards C, Liao L, Laxamana J, Wu B, Swanson S, Song Y, Siguenza P (2024) Immunogenicity of atezolizumab: influence of testing method and sampling frequency on reported anti-drug antibody incidence rates. AAPS J 26(4):84. https://doi.org/10.1208/s12248-024-00954-2
37. Devanarayan V (2016) Interpretation of immunogenicity results and evaluation of clinical associations. Presentation at the European Bioanalysis Forum 9th Open Meeting. https://www.e-b-f.eu/wp-content/uploads/2018/06/bcn2016-D2J4-4-Viswanath-Devanarayan_Abbvie.pdf.
38. van Brummelen EM, Ros W, Wolbink G, Beijnen JH, Schellens JH (2016) Antidrug antibody formation in oncology: clinical relevance and challenges. Oncologist 21(10):1260–1268. https://doi.org/10.1634/theoncologist.2016-0061
39. van Vugt MJH, Stone JA, De Greef R, Snyder ES, Lipka L, Turner DC, Chain A, Lala M, Li M, Robey SH, Kondic AG, De Alwis D, Mayawala K, Jain L, Freshwater T (2019) Immunogenicity of pembrolizumab in patients with advanced tumors. J Immunother Cancer 7(1):212. https://doi.org/10.1186/s40425-019-0663-4
40. Peters S, Galle PR, Bernaards CA, Ballinger M, Bruno R, Quarmby V, Ruppel J, Vilimovskij A, Wu B, Sternheim N, Reck M (2022) Evaluation of atezolizumab immunogenicity: efficacy and safety (part 2). Clin Transl Sci 15(1):141–157. https://doi.org/10.1111/cts.13149